Progress in Microbes and Molecular Biology

HH PUBLISHER

Original Research Article

Immunomodulatory Effects of Phytosterols and Glycosides Derived from *Clinacanthus nutans* in C57BL/6 Mice

Crystal Xiao-Qi Liew[1], Cheng-Foh Le[2], Sui-Kiong Ling[3], Sek-Chuen Chow[4], Li Li Chan[5], Kien Chai Ong[6], Chee-Mun Fang[1]*

Article History

Received: 19 June 2025;

Received in Revised Form: 22 August 2025;

Accepted: 08 September 2025;

Available Online: 11 September 2025

[1]Division of Biomedical Sciences, School of Pharmacy, University of Nottingham Malaysia, 43500 Semenyih, Selangor, Malaysia; crystallxqx@gmail.com (CXQL)

[2]School of Biosciences, University of Nottingham Malaysia, 43500 Semenyih, Selangor, Malaysia; ChengFoh.Le@nottingham.edu.my (CFL)

[3]Natural Products Division, Forest Research Institute Malaysia (FRIM), 52109 Kepong, Selangor, Malaysia; lingsk@frim.gov.my (SKL)

[4]School of Science, Monash University Malaysia, Jalan Lagoon Selatan, 47500 Bandar Sunway, Selangor, Malaysia; Chow.Sek.Chuen@monash.edu (SCC)

[5]Microbiology and Immunology Department, School of Medicine, IMU University, 57000 Kuala Lumpur, Malaysia; lili_chan@imu.edu.my (LLC)

[6]Department of Biomedical Science, Faculty of Medicine, University of Malaya, Federal Territory of Kuala Lumpur, Kuala Lumpur, 50603, Malaysia; kcong@um.edu.my (KCO)

*Corresponding author: Chee-Mun Fang; Division of Biomedical Sciences, School of Pharmacy, University of Nottingham Malaysia, 43500 Semenyih, Selangor, Malaysia; CheeMun.Fang@nottingham.edu.my (CMF)

Abstract: *Clinacanthus nutans* is a traditional medicinal plant widely used in Southeast Asia for its therapeutic properties, including anti-cancer, antimicrobial, and anti-inflammatory effects. While its crude extracts have been studied for immunomodulatory effects, little is known about the effects of its purified compounds. This study examines the immunomodulatory effects of beta-sitosterol, stigmasterol, and shaftoside isolated from *C. nutans* in C57BL/6 mice using immunogenicity tests and an immunosuppressive challenge model. Lymphocyte proliferation was assessed using BrdU assay, spleen immune cell composition was analysed via FACS, and inflammatory cytokines, total IgG, and IgM levels were quantified using ELISA. A *Cryptosporidium parvum* infection model was used to assess immunosuppressive effects in a biologically relevant context. Stool samples were examined microscopically for oocyst counts, and histopathological analysis was performed on the terminal ileum and liver. Shaftoside suppressed B and T lymphocyte proliferation, reduced both Th1 (IFN-γ, IL-2) and Th2 cytokines (IL-4), except IL-10, and altered antibody production by increasing IgG and reducing IgM levels. It also decreased the populations of

key immune cells, including B cells, T helper cells, and cytotoxic T cells. Beta-sitosterol and stigmasterol inhibited lymphocyte proliferation, increased Th1 cytokines and reduced immune cell populations, with beta-sitosterol showing stronger immunomodulatory potential. In the *C. parvum* model, beta-sitosterol mitigated terminal ileum and liver damage more effectively than other treatments but resulted in higher oocyst shedding than dexamethasone. These findings suggest beta-sitosterol's potential as a natural immunomodulatory agent with possible applications in Th2-dominant conditions like asthma and allergies.

Keywords: *Clinacanthus nutans*; beta-sitosterol; stigmasterol; shaftoside; cytokines; immunomodulatory; SDG 3 Good health and well-being

1. Introduction

Herbal remedies have been used for centuries to address inflammation and remain deeply rooted in traditional medicine. As a form of complementary and alternative therapy, herbal medicine is widely utilised worldwide in disease treatment[1]. Despite the widespread use of synthetic drugs, concerns over their adverse effects, including allergic reactions and gastrointestinal issues, have driven interest in natural alternatives[2]. The integration of traditional herbal medicines into modern medical treatments has grown tremendously in recent years. This transformative trend is propelled by the growing recognition of the therapeutic benefits of herbal remedies, not only in mitigating adverse effects associated with synthetic drugs such as non-steroidal anti-inflammatory drugs (NSAIDs) but also in enhancing treatment outcomes[3,4]. Popular medicinal plants such as *Artemisia annua* (artemisia), *Curcuma longa* (turmeric), *Glycyrrhiza glabra* (liquorice), *Zingiber officinale* (ginger), and *Allium sativum L.* (garlic) have been widely used to treat autoimmune and inflammatory diseases[5,6]. For instance, artemisinin isolated from *A. annua* has not only been recognised as the most effective drug with minimal side effects in malaria treatment, but new artemisinin derivatives have also shown potent anti-inflammatory and immunoregulatory effects on autoimmune diseases like systemic lupus erythematosus and multiple sclerosis[7]. Therefore, exploring natural compounds with potential therapeutic applications in the field of immunology is of particular significance.

Southeast Asia is renowned for its abundant plant diversity attributed to the varied tropical climate in this region that fosters the growth of various herbal plants. The traditional use of these plants is deeply rooted in cultural practices, with knowledge often passed down through generations[8]. *Clinacanthus nutans* (Burm. f.) Lindau, a medicinal plant originating from the *Acanthaceae* family, is native to Malaysia, Thailand, Indonesia, and China[9]. *C. nutans* (CN) has been used as a traditional remedy to treat skin rashes, fever, diabetes, and

lesions caused by herpes simplex virus (HSV)[10,11]. This medicinal plant even topped the list on the usage of fresh medicinal plants where users generally consume the plant to boost the immune system, general detoxification, health promotion, cancer treatment, and prevent relapse[12].

CN contains a rich variety of secondary metabolites, including flavonoids, saponins, triterpenoids, diterpenes, phytosterols, and glycosides[13]. Additionally, vital phytochemicals that have been discovered and isolated from CN include stigmasterol (St), beta-sitosterol (Bs), lupeol, vitexin, shaftoside (Sh), orientin, sulphur-containing glucosides, glycoglycerolipids, and monoacylmonogalactosylglycerol[11,14]. Beta-sitosterol, Bs ($C_{29}H_{50}O$) is a phytosterol structurally similar to cholesterol. This compound is a significant member of the phytosterol group and is abundant in nuts, seeds, grains, and vegetable oil[15]. It exhibits anti-inflammatory, antioxidant, anti-cancer, anti-diabetic, and immunomodulatory properties[16]. Moreover, recent molecular docking studies suggest its potential in enhancing immunity against COVID-19 and limiting viral invasion, highlighting its promise in natural health products[17]. Stigmasterol, St ($C_{29}H_{48}O$) is a phytosterol structurally similar to Bs but differs by a double bond at position C-22[18]. It was the first identified chemical compound isolated from CN extract[19]. Extensive research conducted on St has uncovered its diverse pharmacological properties, including anti-cancer, antioxidant, anti-inflammatory, and immunomodulatory activities[20]. Shaftoside, Sh ($C_{26}H_{28}O_{14}$) or schaftoside, is a c-glycosyl flavonoid naturally present in flowers, fruits, vegetables, and leaves. Nowadays, flavonoids are widely used in pharmacological, nutraceutical, cosmetic, and medicine applications due to their broad spectrum of health benefits[21]. C-glycosyl flavones possess many pharmacological properties, including antioxidant, anti-inflammatory, antidiabetic and hepatoprotective activities[22].

The exploration of CN extracts' immunomodulatory effects has been predominantly conducted through in vitro models. The immunomodulatory effect of CN methanol extract on porcine peripheral blood mononuclear cells was found with a significant reduction in IL-10 cytokine mRNA expression[23]. Pro-inflammatory condition in co-cultured breast cancer cells (MDA-MB-231) with human macrophage cells (THP-1), showed significant improvement following treatment with CN extracts with decreased IL-1β and TNF-α cytokine expression[24]. Additionally, Bs from CN's hexane fraction significantly suppressed T cell proliferation, particularly helper and cytotoxic T cells, while reducing Th2 cytokines (IL-4, IL-10) but maintaining Th1 cytokines (IL-2, IFN-γ) in murine splenocytes. This highlights Bs's potential to restore Th1/Th2 balance and modulate an impaired immune system response[25]. However, to our knowledge, there is limited information on the in vivo

immunomodulatory activity of CN, with only one study reported involving a hepatocarcinoma (HepA) model in mice. Huang et al. reported that CN ethanol extract increased IFN-γ and IL-2 while reducing IL-4 in HepA-bearing mice. Spleen analysis showed a decrease in IL-4^+ $CD4^+$ T cell numbers and an increase in IFN-γ^+ $CD4^+$ T cell numbers, while TNF-α and IL-10 remained unchanged[26]. These findings suggest CN extract promotes a Th1-skewed immune response as IFN-γ and IL-2 are major Th1 cytokines, indirectly enhancing anti-tumour effects.

Despite extensive research on CN, most studies focus on whole extracts rather than isolated compounds. The immunomodulatory effects of Bs, St, and Sh remain understudied. This study investigates their immunomodulatory effects in a murine model, building on prior in vitro findings of CN phytosterols' immunosuppressive activity[25]. Studying isolated bioactive compounds from herbal plants like CN is crucial to validate and distinguish their specific therapeutic effects from those traditionally attributed to whole plant extracts[27,28]. This research complements Malaysia's broader efforts in natural product discovery, particularly in advancing therapeutic development from bioactive compounds of natural origin[29]. Hence, the potential implications of this research span the realms of traditional medicine, and the development of novel immunotherapeutic drugs sourced from natural origins.

2. Materials and Methods

2.1. Animal Ethics Approval

Ethical approval for this study was conducted and approved according to the Animal Welfare & Ethical Review Body, University of Nottingham, UK (Ref: UNMC 24), Monash University Malaysia (Project ID: 22105) and International Medical University animal ethics guidelines (Ref: IMU R267/2021).

2.2. Animals

Female C57BL/6 mice (6–8 weeks old) from Monash University Malaysia were used in this study, as female mice are generally less aggressive and easier to group-house compared to males, reducing stress-related variability in experimental outcomes. These mice were housed in individually ventilated cages (treatment phase) and open cages (challenge study). The mice were maintained under controlled conditions (27 ± 2°C, 70–80% humidity, 12 h light/dark cycle), fed with standard mice pellets and water *ad libitum*.

2.3. Preparation of Compounds

The extraction, isolation, and purification of beta-sitosterol (Bs), stigmasterol (St) and shaftoside (Sh) (Figure 1) from the hexane fraction of *Clinacanthus nutans* methanolic extract were performed as previously described[25]. In the present study, structurally identical β-sitosterol and stigmasterol were purchased from commercial suppliers, Bs (CFN99916, purity >=98%, Chemfaces, China), St (CFN97326, purity >=98%, Chemfaces, China), and dexamethasone (D829854, Macklin, China) to ensure sufficient quantity and consistency for downstream experiments. Sh was purified from CN via column chromatography (MCI gel CHP 20P, Sephadex LH-20, Chromatorex ODS, silica gel). The purity of Sh was assessed by high-performance liquid chromatography (HPLC), ranged between 81.3% to 95.9%, and its structural identity was confirmed by nuclear magnetic resonance (NMR) spectroscopy at the Forest Research Institute Malaysia (FRIM), where the purification was performed. Compounds were dissolved in 5% dimethyl sulfoxide (DMSO) (Fisher Scientific, UK) to prepare stock solutions, which were then diluted with phosphate-buffered saline (PBS) prior to experimental use.

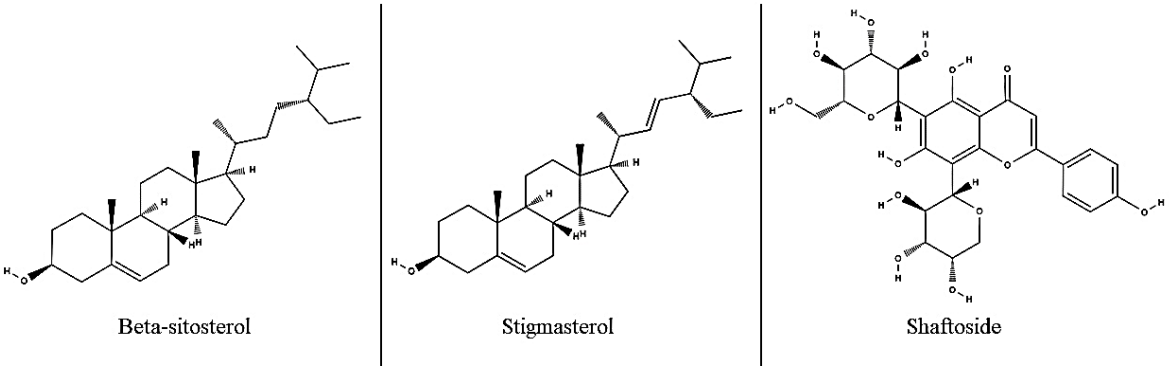

Figure 1. Chemical structure of beta-sitosterol, stigmasterol, and shaftoside.

2.4. Treatment

Mice were assigned to seven groups: control (PBS) and two dosage groups (25 mg/kg, 100 mg/kg) of Bs, St, and Sh (*n*=5/group). The doses were selected based on published toxicity data[14] and our pilot acute oral toxicity study to ensure both safety and pharmacological relevance, with 25 mg/kg representing a conservative sub-therapeutic level and 100 mg/kg reflecting a moderate non-toxic exposure. Oral treatments were given daily for 14 days (0.2 mL per mouse). Body weights and blood samples were collected on days 0, 7, and 14. Mice were euthanised after 14 days with isoflurane and cervical dislocation;

spleens were removed and stored in ice-cold RPMI-10 medium (Corning, USA) for immunogenicity tests.

2.5. Immunogenicity Tests

2.5.1. Single splenocytes suspension preparation

Spleens were homogenised using frosted microscope slides, suspended in RPMI-10 medium and centrifuged (300 × g, 10 min, 4°C). Pelleted splenocytes were further suspended in Ammonium-Chloride-Potassium (ACK) lysis buffer and incubated at RT for 1 min. Splenocytes were washed with 1X PBS and centrifuged (500 × g, 10 min, 4°C), this washing step was repeated. Pelleted splenocytes were suspended in RPMI-10 medium and filtered through a 40 µm nylon cell strainer (SPL Life Sciences, Korea) to obtain a single-cell suspension.

2.5.2. Splenocyte culture and stimulation

Cultures were incubated (72 h, 37°C, 5% CO_2), then used for lymphocytes proliferation assays, FACS, and ELISA. A single splenocyte suspension was used for T cells and B cells stimulations. Cells were seeded at 2×10^6 cells/mL in a sterile, flat-bottomed 6-well plate. T cells and B cells were stimulated with 5 µg/mL of concanavalin A (ConA) and 2 µg/mL lipopolysaccharides (Sigma-Aldrich, USA), respectively. Cultures were incubated (72 h, 37°C, 5% CO_2), then used for proliferation assays.

2.5.3. 5-bromo-2'-deoxyuridine (BrdU) proliferation assay

Splenocyte proliferation of immunised mice was determined using a bromodeoxyuridine (BrdU) colorimetric ELISA kit according to the manufacturer's instructions (Roche Applied Science, USA). Splenocytes were prepared as described above. Absorbance was read at 370 nm (reference: 492 nm). Stimulation index (SI) = A_{370} stimulated / A_{370} untreated. All experiments were performed in three independent trials. Results were reported as relative proliferation (RP) ± SEM.

2.5.4. Cytokine ELISA

Cytokine (IFN-γ, IL-2, IL-4, IL-10) in culture supernatants were measured using BD OptEIA Mouse ELISA kits according to the manufacturer's protocol (BD Biosciences, USA). Splenocyte culture supernatants were prepared as described earlier. Absorbance at 450 nm (reference: 570 nm) was recorded. All experiments were performed in three independent trials. Results were expressed as concentration (pg/mL) ± SEM.

2.5.5. Total IgG & IgM ELISA

Mice blood samples were centrifuged (2000 × g, 10 min, 4°C) to obtain serum. Total IgG and IgM antibody levels in mouse sera were determined using ELISA on anti-IgG/IgM coated plates. Briefly, 96-well flat, maxi-binding immunoplates were coated overnight at 4°C with 100 µL of anti-mouse IgG (1 mg/mL; M8642, Sigma-Aldrich, USA) or anti-mouse IgM (1 mg/mL; SA5-10294, Invitrogen, USA) antibodies, each diluted 1:2000 in 0.1 M Sodium Carbonate buffer. After three washes with washing buffer, plates were blocked with 200 µL of assay diluent for 1 hour at RT, followed by another wash step. Diluted serum samples were added to the appropriate wells and incubated for 2 hours at RT. Plates were then washed six times and incubated with 100 µL of detection antibodies HRP-conjugated goat anti-mouse IgG (1:1000; SC-2005, Santa Cruz Biotechnology, USA) or IgM (1:2000; 62-6820, Invitrogen, USA) in assay diluent for 1 hour at RT. After a final six washes, 100 µL of TMB substrate (BD Biosciences, CA, USA) was added and incubated for 15 minutes at RT in the dark. The reaction was stopped with 2 N sulfuric acid, and absorbance at 450 nm (reference: 570 nm) was recorded. All samples were run in duplicate. Negative (assay diluent) and positive (pooled sera from untreated control mice) controls were included in each assay. Antibody titres were determined using standard curves and expressed as ELISA U/mL, calculated from the inverse of the dilution yielding an absorbance of 0.2 above the blank.

2.5.6. Fluorescent-activated cell sorting (FACS) analysis

Antigen-stimulated splenocytes were prepared as described above. A total of 1×10^6 cells per sample was aliquoted in 25 µL of 1X staining buffer. Each sample was blocked with 1 µg of Mouse BD Fc Block (BD Biosciences, USA) and 10% (v/v) rat serum (Sigma-Aldrich, USA) in staining buffer, followed by incubation on ice for 30 minutes in the dark. After blocking, fluorescent-labelled antibodies were added to the respective samples and incubated for another 30 minutes under the same conditions. The antibodies used for surface marker detection were as follows: PerCP-Cy5.5-labelled anti-mouse $CD4^+$ (Clone RM4-5, 1:800), BB515-labelled anti-mouse $CD8a^+$ (Clone 53-6.7, 1:400), and PE-labelled anti-mouse $CD19^+$ (Clone 1D3, 1:800), all from BD Biosciences (USA). After staining, cells were washed with 1X PBS and centrifuged (500 × g, 5 min, 4°C). The supernatant was discarded, and cells were fixed in 2% (v/v) paraformaldehyde (Nacalai Tesque, Japan) for 10 minutes at RT. A final centrifugation (1800 × g, 5 min, 4°C) was performed, and the cell pellet was resuspended in 1X PBS. Fluorescence data were acquired using the BD Accuri C6 cytometer and BD Accuri C6 software (BD Biosciences, USA).

2.6. Immunosuppressive Challenge Study

Mice were divided into five groups: untreated, Bs, St, Sh (100 mg/kg), and drug control dexamethasone. Compounds for the treatment groups were prepared as described in Section 2.3. The treatment protocol used is as shown in Section 2.4. Bs, St, and Sh were orally administered. Dosage of dexamethasone was at 0.25 mg/kg[30] and was administered *ad libitum* by drinking water[31,32]. Mice were sacrificed on day 30, dissected to retrieve the terminal ileum and liver and secured in 10% buffered formalin (Thermo Fisher Scientific, USA) for histopathological examination.

2.6.1. Infection of oocysts

Cryptosporidium parvum oocysts were administered on the next day after 14 days of treatment with Bs, St, Sh, and dexamethasone. Protocol from Abdou et al. was modified and used in this study[30]. Purified *C. parvum* oocysts (bovine origin) were purchased from the *Cryptosporidium* Production Laboratory (University of Arizona, USA) and orally inoculated with 1×10^5 oocysts in 0.2 mL PBS. Body weight of mice was recorded every 2 days throughout the 30 days challenge study.

2.6.2. Stool examination

Fresh stool pellets were collected from each mouse in the assigned groups every 2 days. Each stool sample group was weighed and recorded, then suspended in 1 mL of 10% buffered formalin and homogenised. One loop of homogenised stool sample (10 µL) was smeared onto a glass slide coated with poly-L-lysine and air-dried. Smears were stained using the modified Ziehl-Neelsen method developed by the United Kingdom National External Quality Assessment Service (UK NEQAS) and examined under a microscope. *Cryptosporidium* oocysts per mg for each group were counted in 10 high-power fields (HPF) as below.

2.6.3. Histopathology

Terminal ileums and livers were processed at the Laboratory of Histopathology in University Malaya. Organs were washed with cold normal saline, fixed in 10% buffered formalin for at least 48 hours, then cut and processed using a standard tissue fixation protocol. Tissues were embedded and sectioned (5 µm) using a rotary microtome, then mounted on glass slides. Slides were stained with Haematoxylin and Eosin (H&E) stain and observed under an Olympus-CX31 light microscope. Severity of infection for the ileum was graded on the villi structures while the liver was assessed on hepatocyte changes and inflammation.

2.7. Statistical Analysis

Data were analysed using GraphPad Prism software. ANOVA with Dunnett's post hoc test was applied. Results were considered significant at $p < 0.05$. Statistics with $p < 0.05$ are denoted with *, $p < 0.01$ with **, and $p < 0.001$ with *** in the graphs.

3. Results

3.1. Immunogenicity Tests

3.1.1. Lymphocytes proliferation assay (BrdU)

T lymphocyte proliferation in ConA-stimulated splenocytes exhibited a reducing pattern across all compounds treated groups (Figure 2). The dashed line indicates there was no difference in proliferation between the co-treatment groups of CN compounds and mitogen alone. Bs-treated mice demonstrated the least suppression (Bs25: 0.53 ± 0.22; Bs100: 0.44 ± 0.23), with no statistical significance. St and Sh groups showed significant suppression (St25: 0.22 ± 0.10, St100: 0.11 ± 0.06; Sh25: 0.14 ± 0.08, Sh100: 0.28 ± 0.10). LPS-induced B lymphocytes proliferation was also suppressed, with Sh groups showing the strongest significant inhibition (Sh25: 0.36 ± 0.04, Sh100: 0.40 ± 0.05), while St25 slightly increased proliferation (1.20 ± 0.13).

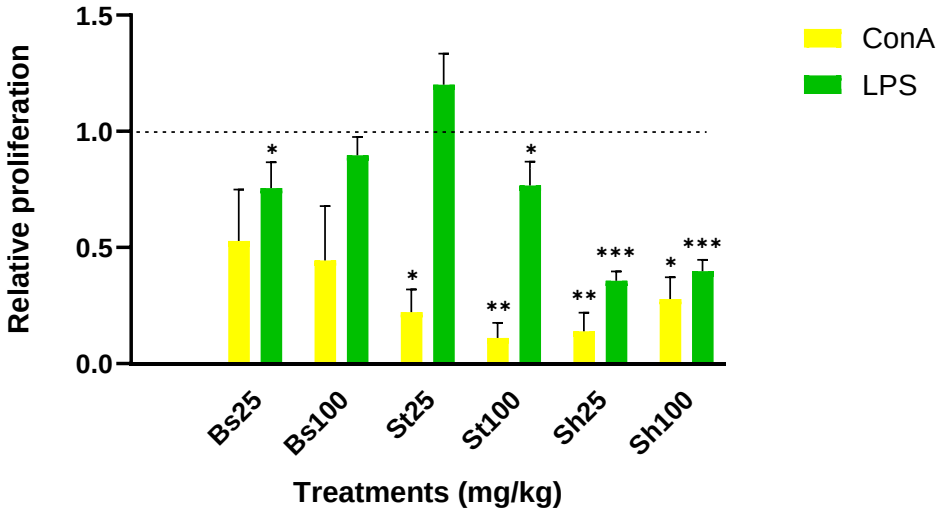

Figure 2. Proliferation profile of splenocytes stimulated with ConA and LPS after treatment measured using BrdU assay. Splenocytes stimulated with 5 µg/mL of ConA and 2 µg/mL of LPS after treatment with CN purified compounds were measured using BrdU assay. The relative proliferation was calculated as the ratio of stimulation index (SI) of co-treatment groups (CN purified compounds + mitogen) against SI of control treated with mitogen alone. Results indicate mean of triplicates and expressed as Relative Proliferation ± S.E.M. Statistical analysis was performed using one-way ANOVA followed by Dunnett's test to compare treatment groups against the untreated control. *$p < 0.05$, **$p < 0.01$, ***$p < 0.001$.

3.1.2. IL-2, IFN-γ, IL-4, and IL-10 Cytokine ELISA

ConA stimulation elevated all cytokine levels in control splenocytes (Figure 3). Most treatments exhibited dose-dependent cytokine inhibition. Sh100 group showed the highest suppression of IFN- γ (20.93 ± 18.24 pg/mL) (Figure 3A), IL-2 (36.37 ± 13.07 pg/mL) (Figure 3B), and IL-4 (15.0 ± 5.42 pg/mL) (Figure 3C) but increased IL-10 (202.82 ± 95.01 pg/mL) (Figure 3D), though not statistically significant. Notably, only IL-2 changes were statistically significant across groups. Sh25 exhibited slightly weaker inhibition of IL-2 and IL-10 but had the greatest IL-10 suppression (31.11 ± 33.89 pg/mL), comparable to the ConA control (33.65 ± 34.21 pg/mL), and a slight stimulation of IFN- γ cytokine (31.28 ± 22.96 pg/mL).

Bs and St groups stimulated cytokine production in a dose-dependent manner. Compared to the ConA control, both Bs groups increased IFN-γ (Bs25: 50.87 ± 0.94 pg/mL, Bs100: 45.34 ± 12.09 pg/mL), IL-2 (Bs25: 234.10 ± 25.47 pg/mL, Bs100: 213.03 ± 15.76 pg/mL), IL-4 (Bs25: 38.92 ± 2.03 pg/mL, Bs100: 34.20 ± 2.31 pg/mL), and IL-10 (Bs25: 84.93 ± 49.37 pg/mL, Bs100: 63.02 ± 33.89 pg/mL) cytokine levels. Similarly, St25 and St100 followed the same trend. Compared to the ConA control, both St groups increased IFN-γ (St25: 44.89 ± 8.30 pg/mL, St100: 38.16 ± 16.37 pg/mL), IL-2 (St25: 209.47 ± 15.76 pg/mL, St100: 139.21 ± 12.61 pg/mL), IL-4 (St25: 39.99 ± 4.21 pg/mL, St100: 34.31 ± 4.21 pg/mL), and IL-10 (St25: 66.11 ± 33.89 pg/mL, St100: 48.73 ± 33.84 pg/mL) cytokine levels. Notably, lower doses (25 mg/kg) of Bs, St, and Sh stimulated cytokine levels more than higher doses (100 mg/kg), except for Sh100, which increased IL-10. These findings suggest that lower CN-purified compound doses may enhance cytokine responses in ConA-stimulated splenocytes.

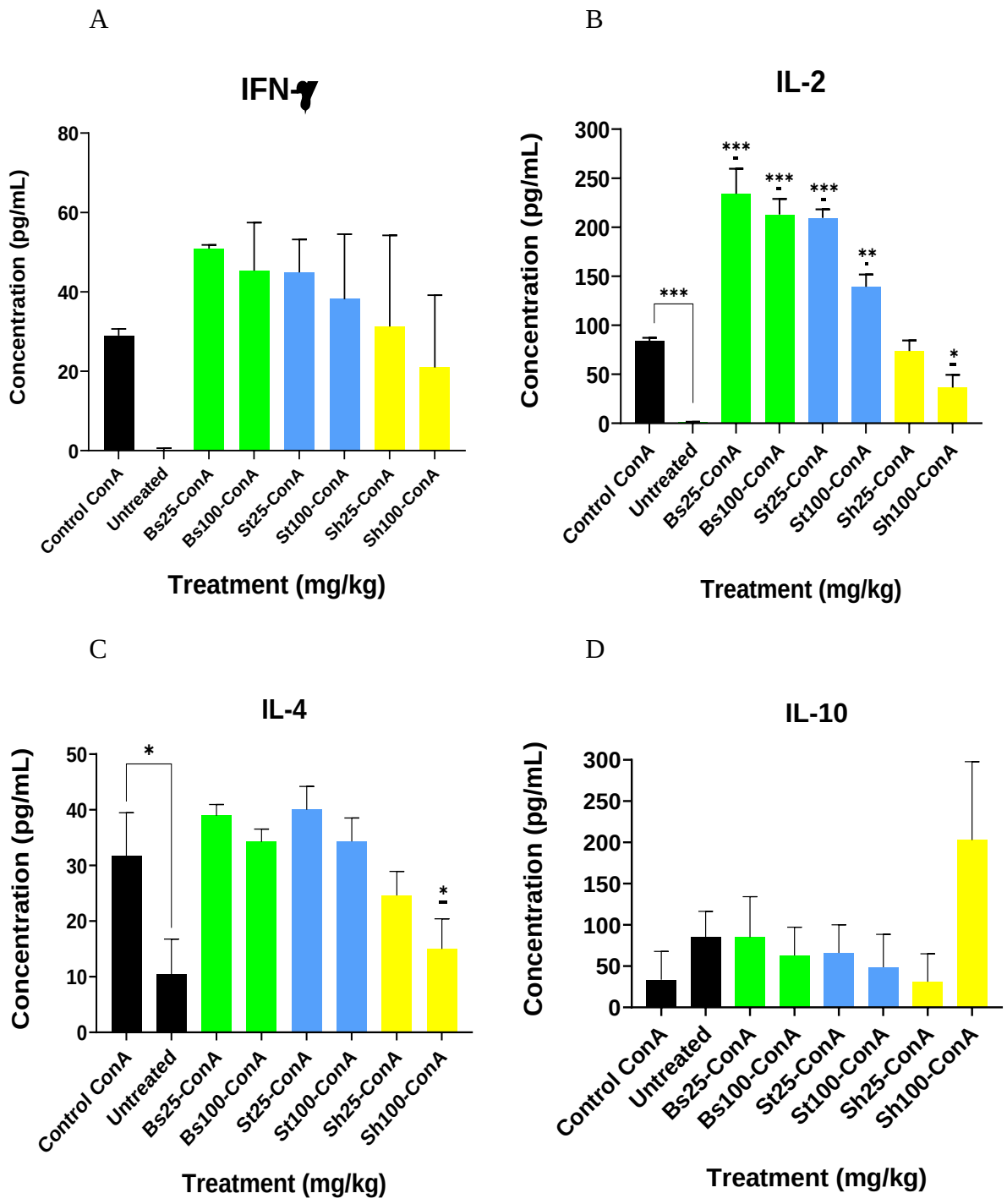

Figure 3. Cytokine secretion levels of C57BL/6 mice treated with Bs, St, and Sh stimulated with ConA measured using ELISA. Splenocytes of C57BL/6 mice treated with Bs, St, and Sh stimulated with ConA were used to measure IFN- γ (A), IL-2 (B), IL-4 (C), and IL-10 (D) cytokine levels using ELISA. Results indicate mean of triplicates and were expressed as concentration (pg/mL) ± S.E.M (n = 5/group). Statistical analysis was performed using one-way ANOVA followed by Dunnett's test to compare treatment groups against the ConA control. *$p < 0.05$, **$p < 0.01$, ***$p < 0.001$.

3.1.3. Total IgG and IgM Antibody Titres

Serum samples from days 0, 7, and 14 were analysed for total IgG and IgM levels (Figure 4A). On day 0, Bs25 had the lowest total IgG ($1.14 \times 10^7 \pm 2.28 \times 10^6$ EU/mL) and St100 had the highest ($3.09 \times 10^7 \pm 2.15 \times 10^7$ EU/mL) compared to the control ($1.75 \times 10^7 \pm 5.79 \times 10^6$ EU/mL). By day 7, all treatment groups surpassed the control mice group ($2.03 \times 10^7 \pm 3.66 \times 10^6$ EU/mL), with St25 demonstrating the lowest ($2.05 \times 10^7 \pm 2.77 \times 10^6$ EU/mL) and St100 with the highest concentration ($3.82\times 10^7 \pm 4.77 \times 10^6$ EU/mL). On day 14, IgG levels in Bs25, Bs100, and St100 remained higher than control ($2.38 \times 10^7 \pm 4.57 \times 10^6$ EU/mL), while St25, Sh25, and Sh100 were lower. St100 had the highest IgG ($3.11 \times 10^7 \pm 4.40 \times 10^6$ EU/mL), while Sh100 had the lowest ($1.64 \times 10^7 \pm 2.20 \times 10^6$ EU/mL). Overall, the untreated control mice group displayed a gradual increase in antibody titres from day 0 to day 14, whereas treatment groups exhibited dynamic trends. Although the measured total IgG antibody levels were not statistically significant, Bs and Sh treatments generally increased IgG over time, while St-treated mice showed a dose-dependent IgG rise. Notably, Bs25 showed a stronger upward trend in IgG than Bs100 at later time points, suggesting a possible dose-dependent effect.

Total IgM levels in treatment and control groups are shown in Figure 4B. On day 0, Bs25 had the lowest IgM ($3.86 \times 10^4 \pm 1.63 \times 10^4$ EU/mL, $P \leq 0.02$) and Sh100 the highest ($1.86 \times 10^5 \pm 3.80 \times 10^4$ EU/mL, $P \leq 0.05$) compared to the control ($1.17 \times 10^5 \pm 3.02 \times 10^4$ EU/mL). By day 7, Bs25, Sh25, and Sh100 showed increased IgM, while Bs100, St25, and St100 had lower levels. Among treatments, Bs100 had the lowest ($8.23 \times 10^4 \pm 3.02 \times 10^3$ EU/mL) and Sh25 the highest ($1.43 \times 10^5 \pm 1.72 \times 10^4$ EU/mL), though differences were not statistically significant. On day 14, Bs25, Bs100, and St25 had higher IgM than the control ($1.17 \times 10^5 \pm 1.89 \times 10^4$ EU/mL), while St100, Sh25, and Sh100 had lower levels. Sh100 had the lowest ($4.56 \times 10^4 \pm 3.80 \times 10^3$ EU/mL, $P \leq 0.03$), while Bs25 had the highest ($1.48 \times 10^5 \pm 1.26 \times 10^4$ EU/mL). Control mice maintained stable IgM levels, whereas Bs-treated groups showed similar trends in both IgG and IgM, with greater elevation at lower doses. St groups exhibited consistent IgM suppression, with greater reductions at higher doses and a transient response at lower doses, while Sh groups showed a dose-dependent IgG and IgM decline.

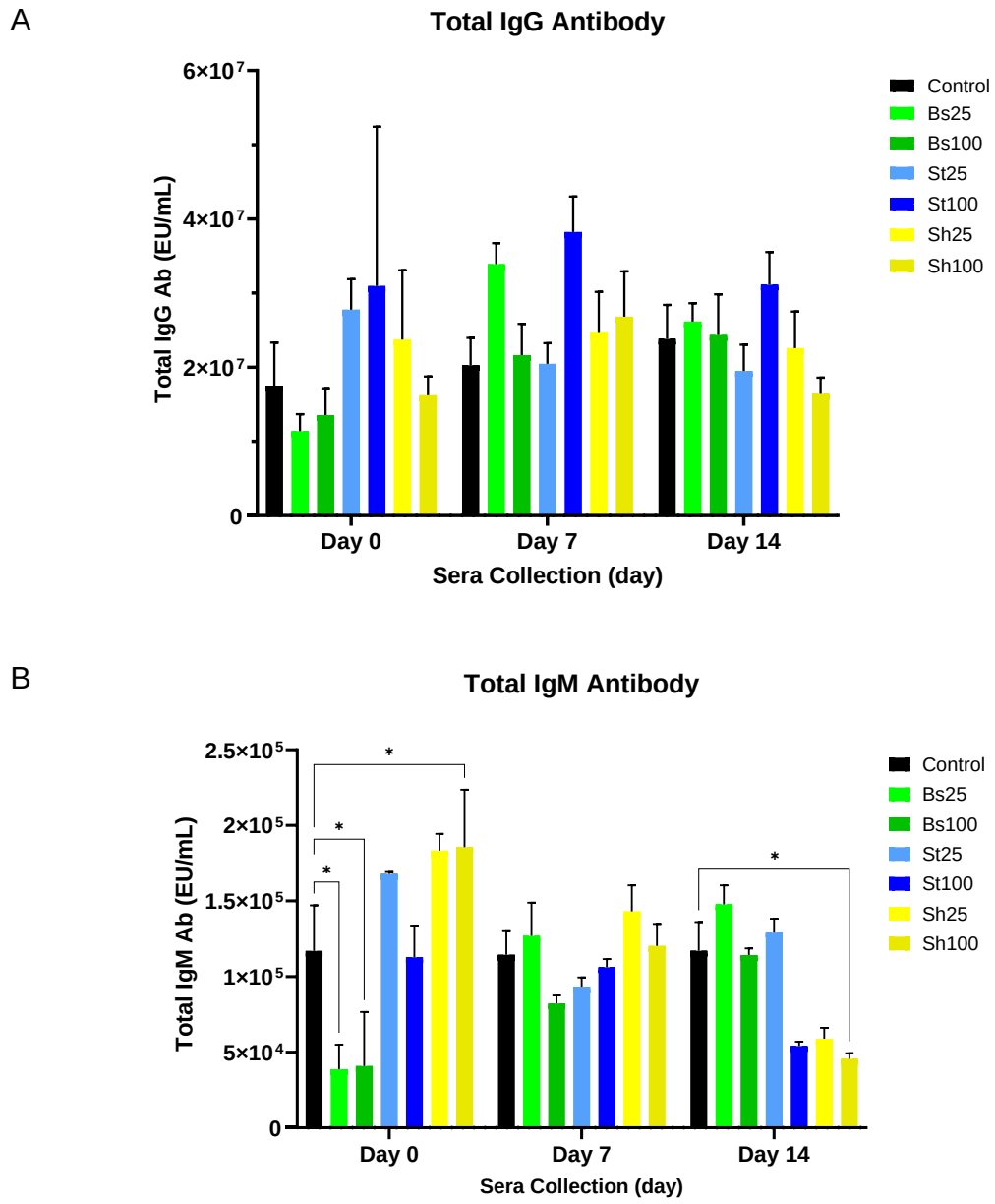

Figure 4. Total IgG and IgM antibody levels in the serum of C57BL/6 mice measured during treatment with Bs, St, and Sh using ELISA. Serum of C57BL/6 mice collected on days 0, 7, and 14 were measured using ELISA to examine the total IgG and IgM levels during treatment with Bs, St, and Sh at low dose 25mg/kg and high dose 100 mg/kg. Results indicate mean of duplicates and were expressed as concentration in ELISA unit (EU/mL) ± S.E.M (n = 5/group). Statistical analysis was performed using one-way ANOVA followed by Dunnett's test to compare treatment groups against the untreated control. *$p < 0.05$.

3.1.4. B cells and T cells population (FACS)

Mice splenocytes stimulated with ConA and LPS were measured for the B cells ($CD19^+$) and T cells ($CD4^+$ and $CD8^+$) populations, with percentage based on live cells from 50,000 event counts (Figure 5). No statistically significant changes were observed, but immune cell modulation trends were noted. For ConA-stimulated $CD19^+$ B cells, all treatments showed inhibition, with Bs25 having the strongest effect (45.14 ± 1.73%) and

Bs100 the weakest (57.77 ± 21.08%) compared to control (58.52 ± 3.94%) (Figure 5A). Under LPS stimulation, St25 showed the largest apparent inhibition in $CD19^+$ B cells (27.43 ± 9.69%), followed by Bs100 (28.58 ± 17.76%) (Figure 5B). The other treatments had a similar inhibitory effect on the percentage population of $CD19^+$ B cells. $CD4^+$ T cells were inhibited in all groups under ConA, with Sh25 showing near-complete suppression (Figure 5A). Lower doses (25 mg/kg) generally had stronger inhibitory effects than higher doses (100 mg/kg). Under LPS stimulation, Sh100 showed the greatest reduction (16.21 ± 12.24%) compared to control (18.01 ± 1.94%), while Bs100 increased $CD4^+$ T cells (24.72 ± 19.23%) (Figure 5B). For ConA-stimulated $CD8^+$ T cells shown in Figure 5A, Bs100 appeared to have the strongest inhibition (0.66 ± 0.66%) versus the control (14.56 ± 0.04%) and other treatment mice groups. However, under LPS stimulation, all treatments increased $CD8^+$ T cell populations, with Bs100 showing the largest apparent increase (21.63 ± 4.90%) (Figure 5B). Overall, the observed trends suggest that Bs mice group may reduce $CD8^+$ T cells population, St mice group may target $CD19^+$ B cells while Sh mice group may most effectively suppress $CD4^+$ T cell populations under these experimental conditions. These trends were interpreted cautiously given the lack of statistical significance.

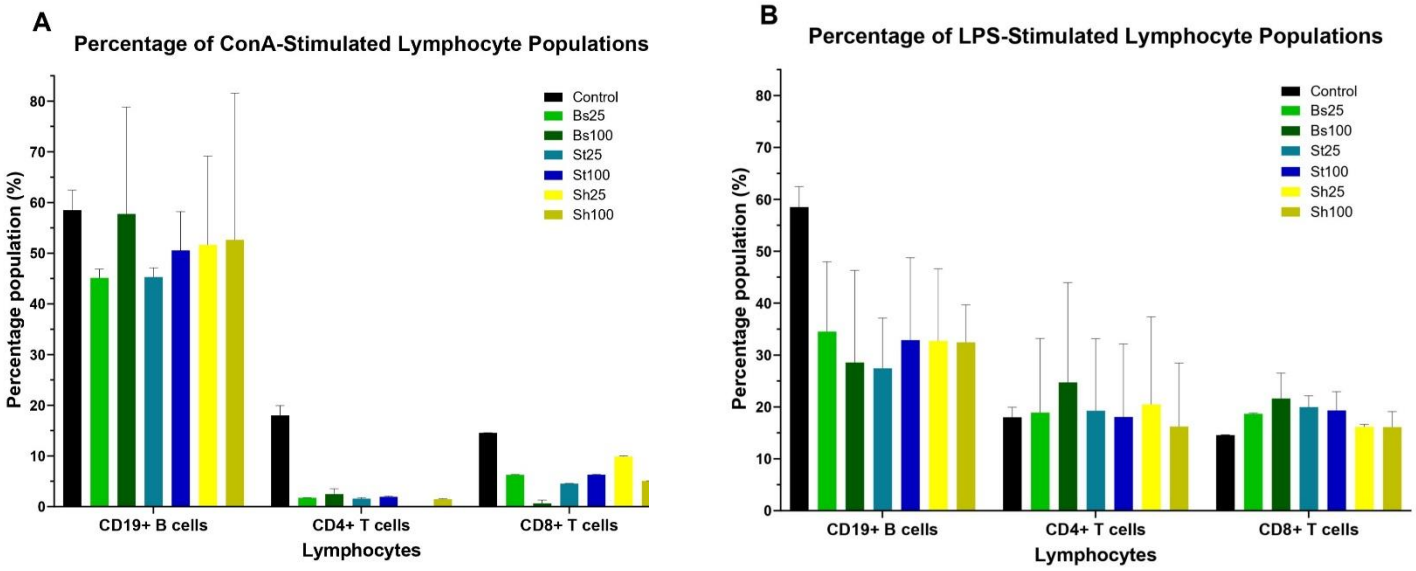

Figure 5. Percentage populations of lymphocytes in murine splenocytes stimulated with ConA and LPS after treatment with Bs, St, and Sh measured using FACS. Murine splenocytes stimulated with 5 µg/mL of ConA (A) and 2 µg/mL of LPS (B) for 72h were stained with fluorescent-labelled antibodies to determine the T cells and B cells populations in C57BL/6 mice treated with 25 and 100 mg/kg of Bs, St, and Sh. The percentage population of CD19+ B cells, CD4+ T helper cells, and CD8+ T cytotoxic cells for each compound were quantified and analysed using FACS. Results indicate mean of duplicates and were expressed as percentage of cells population (%) ± S.E.M (n = 5/group). Statistical analysis was performed using one-way ANOVA with Dunnett's test to compare treatment groups against the untreated control; no significant differences were detected.

3.2. Immunosuppressive Challenge Study

3.2.1. Treatment Weight Changes

Weight gain was observed in all mice groups during the 14-day treatment (Figure 6A). Untreated control mice had the highest increase (day 7: 7.79 % ± 6.35, day 15: 9.4 % ± 6.16).

Bs and St mice groups followed a similar trend (day 7: 5.78 % ± 4.48, 5.87 % ± 3.57; day 14: 5.96 % ± 4.20, 6.06 % ± 3.45, respectively). Sh group showed the greatest weight gain among treatments (day 7: 6.44% ± 5.84, day 14: 7.47% ± 5.99). Dexamethasone group exhibited the most weight loss (day 7: 7.27% ± 4.85, day 14: 2.63% ± 4.09).

3.2.2. Challenge Weight

All groups, including the untreated control, showed weight loss after inoculation, which was most prominent from day 2 onwards (Figure 6B). Dexamethasone group had the greatest weight loss (-11.67% ± 4.92%), followed by control (-8.09% ± 5.11%), Bs (-5.92% ± 2.75%), Sh (-4.85% ± 2.42%), and St (-4.16% ± 3.46%). Bs group was the fastest to regain its initial weight by day 6 (0.30% ± 3.11%), followed by Sh (1.03% ± 3.07%). St and dexamethasone groups recovered by day 8 (1.64% ± 3.46% and 0.90% ± 5.82%, respectively), while the untreated control took the longest, recovering by day 16 (0.70% ± 4.10%). All mice groups gradually regained weight until day 30, indicating recovery from cryptosporidiosis.

3.2.3. Oocyst Count

Higher oocyst shedding indicated immunosuppression, with efficacy compared to dexamethasone. Oocyst shedding peaked on day 4 for control (44.98 ± 1.79), Bs (84.26 ± 3.25), and Sh (58.76 ± 2.15) groups; and on day 6 for St (79.95 ± 2.92) and dexamethasone (107.70 ± 4.81) (Table 1). Dexamethasone-treated mice had the highest shedding. Oocyst counts declined after day 6 and were undetectable by day 12. Control group had the lowest count by day 10 (5.02 ± 0.40), while dexamethasone still had the highest, followed by St, Sh, and Bs groups. Thus, showing that Bs mice cleared oocysts fastest among the treatment groups despite the higher initial load.

Table 1. Table 1. Counts of Cryptosporidium parvum oocysts per HPF in stools of female C57BL/6 mice (n = 5/group) after 30 days of treatment.

Group	**Mean no. of *C. parvum* oocysts /HPF**				
	Day 2	**Day 4**	**Day 6**	**Day 8**	**Day 10**
Untreated control	22.78 ± 0.95	44.98 ± 1.79	22.80 ± 0.50	11.06 ± 1.02	5.02 ± 0.40
β-Sitosterol (100 mg/kg)	$48.59 \pm 1.71^{***\dagger\dagger}$	$84.26 \pm 3.25^{*\dagger\dagger}$	$53.55 \pm 2.05^{*\dagger\dagger\dagger}$	$13.67 \pm 1.11^{**\dagger\dagger}$	$5.29 \pm 0.60^{**\dagger}$
Stigmasterol (100 mg/kg)	$48.28 \pm 1.59^{***\dagger\dagger\dagger}$	$35.23 \pm 0.81^{(NS)\dagger\dagger\dagger}$	$79.95 \pm 2.92^{***\dagger\dagger\dagger}$	$15.56 \pm 0.94^{**\dagger\dagger\dagger}$	$8.17 \pm 1.01^{***\dagger\dagger\dagger}$
Shaftoside (100 mg/kg)	$37.35 \pm 1.46^{***\dagger\dagger\dagger}$	$58.76 \pm 2.15^{***\dagger\dagger\dagger}$	$28.69 \pm 0.45^{***\dagger\dagger\dagger}$	$15.62 \pm 1.30^{**\dagger\dagger\dagger}$	$5.60 \pm 0.46^{**\dagger\dagger\dagger}$
Dexamethasone (0.25 mg/kg)	$33.07 \pm 1.12^{***}$	$55.56 \pm 2.02^{***}$	$107.70 \pm 4.81^{***}$	$18.85 \pm 1.05^{***}$	$9.72 \pm 0.98^{***}$

Data represent mean ± SEM (n = 5/group). Statistical analysis was performed using one-way ANOVA followed by Dunnett's multiple comparison test, analysed separately for each day. Asterisks (*, **, ***) indicate comparisons with the untreated infected control, while daggers (†, ††, †††) indicate comparisons with dexamethasone. Significance levels were set at $p < 0.05$ (* or †), $p < 0.01$ (** or ††), and $p < 0.001$ (*** or †††). NS denotes not significant.

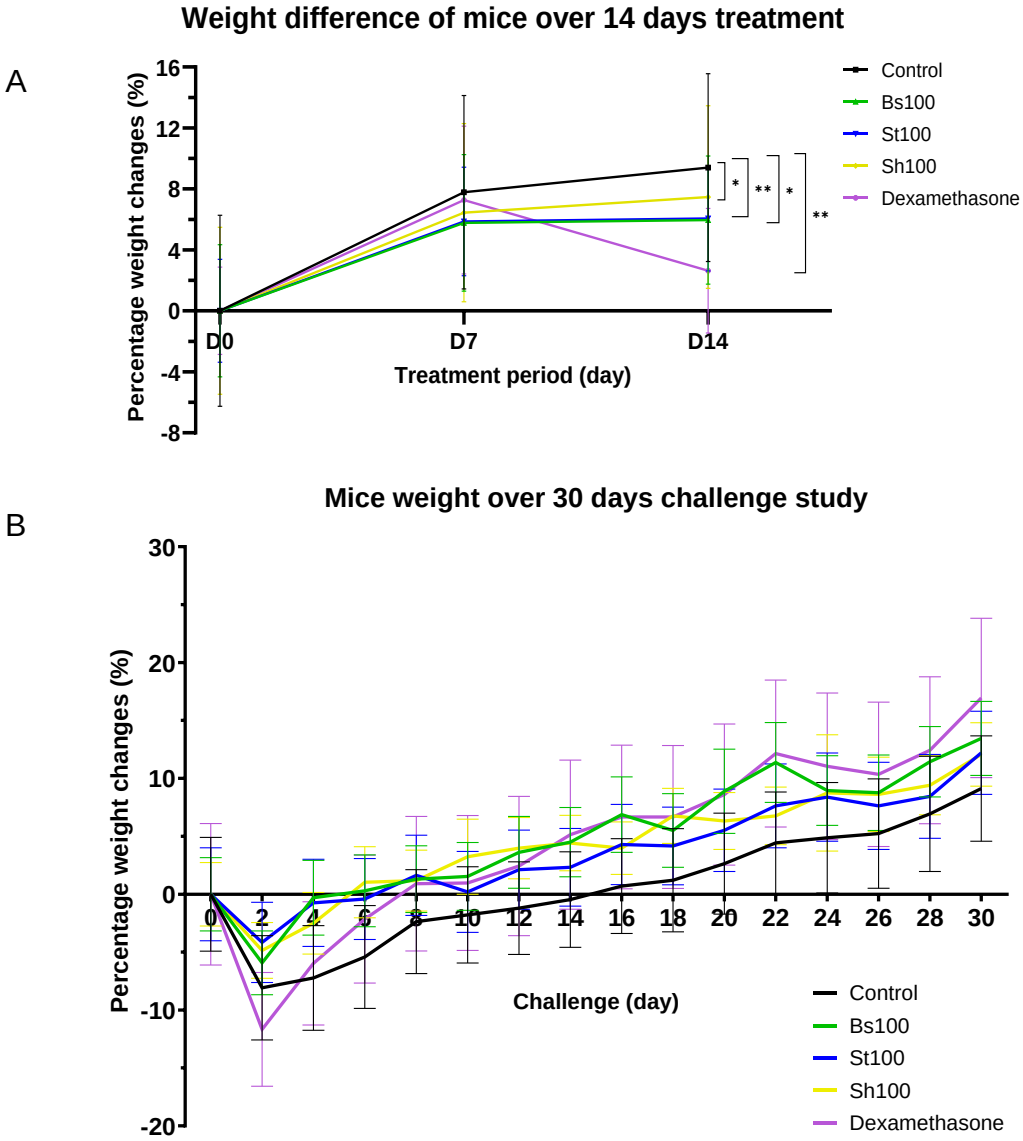

Figure 6. Effects of treatment and *C. parvum* oocyst challenge on body weight changes in female C57BL/6 mice. (A) Percentage of weight change during a 14-day treatment with Bs, St, and Sh. Measurements were taken on days 0, 7, and 14. (B) Percentage of weight change during a 30-day *C. parvum* oocyst challenge study following a 14-day treatment with Bs, St, and Sh, and control drug dexamethasone at 100 mg/kg were recorded every 2 days. Results are expressed as mean percentage weight changes (%) ± SEM (n = 5/group). Statistical analysis was performed using one-way ANOVA followed by Dunnett's test to compare treatment groups against the untreated control. *$p < 0.05$ and **$p < 0.01$.

3.2.4. Histopathological observations

H&E staining revealed structural damage in all treatment groups, graded by severity: control (0), Bs (1), Sh (2), St (3), and dexamethasone (4) (Figure 7). Control mice had normal ileum structure with villi appearing tall, properly lined by columnar and vacuolated epithelial cells (Figure 7A). Bs group showed damaged villi at the tip with disrupted columnar epithelium (Figure 7C). St group exhibited the most severe damage, with shortened villi, disrupted columnar and completely missing epithelial layer (Figure 7E). Sh group had less

extensive damage, with some normal structured villi still intact (Figure 7G). Dexamethasone group showed the most extensive ileum damage, with uniform disruption of villi across the ileum, completely missing epithelial layer, and exposed intestinal crypts (Figure 7I).

Hepatocyte damage severity was highest in dexamethasone, followed by St, Sh, Bs-treated groups, and control (Figure 7). Liver section from control mice showed normal hepatocytes with very minimal focal inflammation and diffuse vacuolation (Figure 7B). Bs group showed focal inflammation, diffused vacuolation of hepatocytes but with additional focal hepatocytes necrosis, represented by the loss of hepatocyte cytologic details (Figure 7D). St group showed several focal inflammations with early infiltration of inflammatory cells and larger areas of diffuse vacuolation associated to fatty change (Figure 7F). Sh group showed similar but less severe inflammation and hepatocyte changes compared to St group (Figure 7H). Dexamethasone group had the most severe inflammation with higher numbers of focal inflammation and larger areas of focal necrosis observed as indicated with pink blurry patches, a distinct characteristic of necrosis due to the loss of hepatocyte cytologic details (Figure 7J).

4. Discussion

The present study investigated the immunomodulatory effects of Bs, St, and Sh, three compounds isolated from *Clinacanthus nutans*, in C57BL/6 mice. These compounds were selected based on our previous in vitro findings demonstrating a Th1-biased immune response in murine splenocytes[25]. The intricate interplay between B and T lymphocytes and their secreted cytokines underlies both humoral and adaptive immunity[33]. Sh demonstrated the most potent immunomodulatory and anti-inflammatory profile, as seen in the BrdU and FACS assays. Notably, the Sh25 group significantly suppressed $CD4^+$ T helper cell in ConA-stimulated splenocytes (Figure 5A). This downregulation of lymphocyte activity coincided with reduced levels of both Th1 (IFN-γ, IL-2) and Th2 (IL-4) cytokines and increased secretion of anti-inflammatory IL-10 at higher doses of Sh (Figure 3). These observations suggest a shift toward a Th2-biased immune environment with anti-inflammatory characteristics. While FACS analysis did not yield statistically significant differences, the trends support Sh's immunomodulatory potential. This limitation may be due to sample size, assay sensitivity, or pharmacodynamic variability. Future studies should aim to increase statistical power by using larger sample sizes and addressing experimental variability. Interestingly, Sh modulated immune parameters relevant to allergic responses. The reduced IL-4 levels, suppression of $CD4^+$ T helper cells, and enhanced IL-10 suggest the compound's potential in attenuating allergic inflammation[34,35]. Additionally, Sh increased total IgG levels and suppressed total IgM in a dose-dependent manner (Figure 4). Moreover, the

relationship between IL-4 suppression, total IgM reduction, and total IgG promotion is complex but not necessarily contradictory. This antibody shift aligns with the class-switching mechanism mediated by IL-4, which promotes IgG and suppresses IgM[36,37]. Reduced IgM could reflect a diminished initial B cells activation, as IgM is often the first antibody produced, while IgG elevation suggests a transition to a more regulated immune state[38]. Collectively, these findings indicate that Sh supports immune modulation by suppressing early immune responses and fostering anti-inflammatory signalling such as dendritic cells[39].

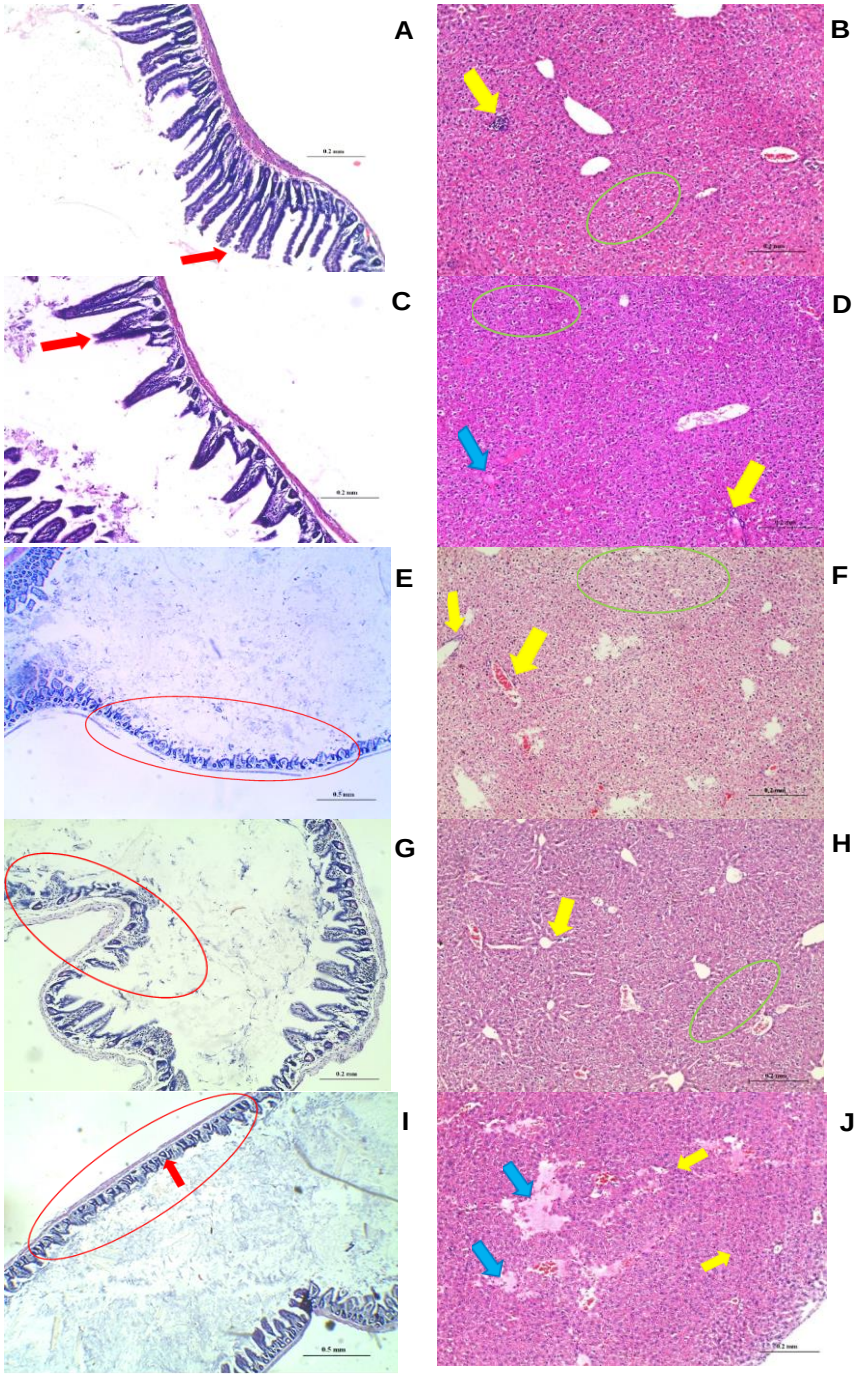

Figure 7. Histopathological observations of the terminal ileum and liver in mice after 30 days of oocyst challenge. (A) Ileum section from an untreated control mouse showing normal villi structure lined by columnar

and vacuolated epithelial cells (red arrow). (B) Liver section from an untreated control mouse showing normal hepatocytes with minimal focal inflammation (yellow arrow) and diffuse vacuolation (green circle). (C) Ileum section from a Bs-treated mouse showing some damaged villi tips (red arrow). (D) Liver section from a Bs-treated mouse showing focal inflammation (yellow arrow), diffuse vacuolation (green circle), and focal hepatocyte necrosis (blue arrow). (E) Ileum section from a St-treated mouse showing extensive villi damage with disrupted columnar and missing epithelial layers (red circle). (F) Liver section from a St-treated mouse showing several focal inflammations (yellow arrow) and diffuse vacuolation (green circle). (G) Ileum section from a Sh-treated mouse showing similar findings to stigmasterol treatment but with less severity (red circle). (H) Liver section from a Sh-treated mouse showing focal inflammation (yellow arrow) and diffuse vacuolation (green circle). (I) Ileum section from a dexamethasone-treated mouse showing uniform disruption of villi structure (red circle) with exposed intestinal crypts (red arrow). (J) Liver section from a dexamethasone-treated mouse showing focal inflammation (yellow arrow) and focal hepatocyte necrosis (blue arrow). All images are stained with H&E, magnified ×100 unless otherwise stated, and have scale bars representing 0.2 mm, except for (E) and (I), which have a magnification of ×40 and scale bars of 0.5 mm.

Bs and St mice groups also displayed potential immunomodulatory effects but with distinct profiles. Both compounds increased Th1 cytokines (IFN-γ, IL-2) in a dose-dependent manner while leaving IL-4 and IL-10 largely unaltered, indicating a Th1-dominant skew. (Figure 3). This agrees with prior studies reporting that Bs suppressed Th2 cytokines (IL-4, IL-10) while maintaining or promoting Th1 cytokines, thereby enhancing the Th1/Th2 ratio[25,40]. This result also aligns with our findings and provides further evidence of the immunomodulatory effects of Bs and St on Th1/Th2 balance. Such a shift could be beneficial in conditions involving Th2 overactivation. The immunomodulatory potential of Bs was further confirmed through FACS analysis, where Bs-treated mice showed decreased populations of $CD4^+$ and $CD8^+$ T cells in ConA-stimulated splenocytes (Figure 5A). This mirrors the effect of compounds like gossypol, which modulate both Th1 and Th2 cytokines to suppress T cell activation[41]. These effects likely occur through interference with transcription factors such as nuclear factor kappa B (NF-κB), calcium-calcineurin-nuclear factor of activated T cell (NFAT) and activator protein 1 (AP-1)[42,43]. Bs also suppressed total IgG and IgM in a dose-dependent manner, suggesting long-term suppression of humoral responses, which is consistent with the observed reduction in B lymphocytes proliferation. (Figure 4).

The immunomodulatory effects of St were more complex. FACS results indicated suppression of $CD4^+$ T cells and $CD19^+$ B cells while simultaneously promoting $CD8^+$ T cells, especially at higher dosages (Figure 5A). This selective modulation implies that St might favour cytotoxic T cell-mediated responses while suppressing helper and humoral components. St also led to increased total IgG and suppressed IgM levels, indicating class switching and immunosuppressive regulation of B cells activity (Figure 4). Interestingly, the St25 group showed limited inhibition of B cells proliferation, possibly due to the sub-therapeutic dose. However, the general trend across other treatment groups, excluding St25, was a consistent suppression of B and T cells proliferation despite mitogenic stimulation by

ConA and LPS. These findings support earlier in vitro work where Bs and St suppressed T lymphocyte proliferation[25]. Furthermore, the reported inhibition of cell cycle progression and its anti-tumour properties of St may contribute to its effects on immune cell proliferation[20]. The immunogenicity results also suggest a dose-dependent modulation of antibody production and lymphocyte activity by St. These results highlight the interconnected effects of the compounds on cytokine secretion, lymphocyte proliferation, and humoral responses, which may be harnessed for therapeutic purposes in immune-related disorders. Natural compounds, including those from CN, may exert immunomodulatory effects through mechanisms such as autophagy modulation, as discussed in recent pharmacological reviews[44]. Given the promising immunomodulatory effects observed with Bs, St, and Sh, further mechanistic evaluation is crucial. This includes elucidating key signalling pathways such as Janus Kinase-Signal Transducer and Activator of Transcription (JAK-STAT), Mitogen-Activated Protein Kinase (MAPK), and NF-κB through gene expression profiling and pathway inhibition assays[45]. Recent modelling-based studies highlight the importance of targeted validation in advancing plant-derived immunomodulatory agents[46].

The infection model using *Cryptosporidium parvum* was incorporated to evaluate the functional relevance of immunosuppression in vivo[47]. Immunosuppressants can compromise host defences, leading to susceptibility to infections. Thus, the infection model provided a physiologically relevant context for assessing the risk-benefit profile of these compounds. Evaluation of compound through an infection model helps identify potential risks associated with immunosuppression, which may not be evident in models of allergic or autoimmune conditions. Additionally, a positive control was not included in the first experiment as the objective was to evaluate the baseline immunomodulatory effects of Bs, St, and Sh in healthy mice without external immune stimulation. However, in the *Cryptosporidium parvum* infection model, dexamethasone was used as a positive control to validate the immunosuppressive effects of these compounds under immune challenge conditions[30]. Moreover, administering dexamethasone *ad libitum* through drinking water is a common method in murine studies, allowing for continuous drug intake with minimal handling stress[48]. While individual water consumption can vary, studies have shown that C57BL/6 mice consume approximately 6 mL of water daily[32]. This consumption rate facilitates the calculation of an average dexamethasone dosage per mouse.

Dexamethasone, a synthetic glucocorticoid, was used as a control drug to induce chemical immunosuppression in mice. Potent immunosuppressive agents may exert systemic effects, reinforcing the need to assess safety profiles of natural immunosuppressants[49]. As expected, dexamethasone-treated mice showed the most significant weight loss, followed by

Sh, St, and Bs groups. All groups lost weight post-infection, reflecting the pathogenic effect of cryptosporidiosis[50]. However, the control group regained weight the fastest, suggesting intact immune function and faster pathogen clearance (Figure 6B). Oocyst count (Table 1) and histopathology examinations (Figure 7A-B) supported this, as the control mice cleared oocyst shedding rapidly and exhibited minimal tissue damage. These findings align with previous reports that oocyst shedding lasts 3–4 weeks, validating our 30-day study duration[51].

Any significant increase or decrease in body weight from the control group is an indicator of adverse effects from the administered substance[52]. No significant weight changes were noted among CN compound-treated mice, apart from transient fluctuations likely due to appetite variations. (Figure 6A). In comparison, dexamethasone consistently led to severe weight loss (Figure 6A and Figure 6B) and the highest oocyst shedding (Table 1). Interestingly, Bs-treated mice exhibited higher oocyst shedding initially but cleared the infection more rapidly than other CN groups, potentially due to enhanced immune modulation over time. This aligns with the observed faster recovery of body weight in the Bs group, indicating a more effective immune response over time. Histological analysis revealed that Bs-treated mice also experienced the least ileal and hepatic damage among treatment groups (Figure 7C-D). Although the control group ultimately exhibited the lowest overall oocyst burden, Bs-treated mice showed the fastest clearance among the treatment groups despite the higher initial load. Coupled with the reduced tissue injury, these findings suggest that Bs offers a comparatively favourable outcome relative to St, Sh, and dexamethasone, though not surpassing the protective effect observed in the untreated control group.

Taken together, these outcomes suggest that Bs exerts immunomodulatory effects that appear to involve immunosuppressive activity, yet with lower histopathological impact, making it a promising candidate for immune modulation with minimal side effects. Phytosterols like Bs and St have been reported to alleviate conditions such as colitis and non-alcoholic fatty liver disease (NAFLD), supporting their anti-inflammatory potential[53,54]. The immunomodulatory effects of CN-derived compounds such as Bs, St, and Sh may also involve underlying cellular mechanisms like autophagy modulation, which has been increasingly recognised as a pathway influencing immune cell function and cytokine regulation[44]. This study provides a descriptive analysis of the immunomodulatory effects of Bs, St, and Sh; however, further investigations are required to elucidate the molecular mechanisms and signalling pathways involved in their immunomodulatory actions. Limitations such as reliance on the single cell line in the earlier in vitro studies and variability in shaftoside purity due to manual extraction may have influenced reproducibility[25,55].

Future studies should incorporate larger sample sizes, explore chronic toxicity profiles, and validate findings in disease-specific models such as autoimmune or allergic conditions[56].

5. Conclusion

In conclusion, this study shed light on the immunomodulatory effects of Bs, St, and Sh, compounds isolated from *Clinacanthus nutans*. These compounds modulated key immune functions, including lymphocyte proliferation, cytokine secretion, and antibody production. Sh demonstrated promising immunomodulatory and anti-inflammatory effects, suppressing B and T lymphocytes proliferation, reducing Th1 and Th2 cytokines (except IL-10), and decreasing IgM while increasing IgG levels. Bs and St exhibited immunomodulatory potential by stimulating Th1 cytokines (IFN-γ, IL-2) in a dose-dependent manner without affecting Th2 (IL-4, IL-10) cytokines. Bs strongly suppressed $CD4^+$ and $CD8^+$ T cells, while St selectively inhibited $CD19^+$ B cells and stimulated $CD8^+$ T cells. In the *Cryptosporidium parvum* infection model, Bs demonstrated modulation consistent with immunosuppressive activity with minimal histological damage, indicating its potential as a safer immunomodulatory agent. Compared to conventional agents such as dexamethasone, which broadly suppressed immunity and caused significant tissue injury, Bs exerted more selective modulation while sparing tissue damage. These findings underscore the therapeutic potential of Bs in conditions that necessitate immune system modulation, such as autoimmune diseases, allergies, or transplant rejection.

Author Contributions: CXQL and C.M.F- Writing original draft and conceptualisation. CFL, SKL, SCC, LLC and KCO- Writing—review and editing. All authors approved the final version of the manuscript.

Funding: This study was supported and funded by Ministry of Higher Education Malaysia (MoHE) through the Fundamental Research Grant Scheme (FRGS). Grant Number FRGS/1/2018/SKK08/UNIM/02/2.

Conflicts of Interest: The authors declare no conflict of interest.

References

1. B K, Babu AK, Pillay SM, *et al*. A Review of Herbal Treatment for Functional Gastrointestinal Disorders and Infection. Prog Microbes Mol Biol 2023;6(1). Available from: https://journals.hh-publisher.com/index.php/pmmb/article/view/875
2. Sobhani K, Li J, Cortes M. Nonsteroidal Anti-inflammatory Drugs (NSAIDs). StatPearls Publishing; 2023. Available from: https://www.ncbi.nlm.nih.gov/books/NBK547742/
3. Chatterjee A, Bandyopadhyay SK. Herbal Remedy: An Alternate Therapy of Nonsteroidal Anti-Inflammatory Drug Induced Gastric Ulcer Healing. Ulcers 2014;2014:1–13.
4. Ji J, Phang HC, Gu X, *et al*. A Review on Colorectal Cancer and the Role of Traditional Chinese Herbal Medicine as Complementary Therapy. Prog Microbes Mol Biol 2024;7(1). Available from: http://journals.hh-publisher.com/index.php/pmmb/article/view/1073
5. Sahoo BM, Banik BK. Medicinal plants: source for immunosuppressive agents. Immunol Curr Res

2018 [cited 2020 May 21];2(1):106. Available from: https://www.researchgate.net/publication/328602864

6. Lim WQ, Cheam JY, Law JWF, Letchumanan V, Lee LH, Tan LTH. Role of Garlic in Chronic Diseases: Focusing on Gut Microbiota Modulation. Prog Microbes Mol Biol 2022;5(1). Available from: https://journals.hh-publisher.com/index.php/pmmb/article/view/655

7. Shi C, Li H, Yang Y, Hou L. Anti-inflammatory and immunoregulatory functions of artemisinin and its derivatives. Mediators Inflamm 2015;2015.

8. Kalusalingam A, Kamal K, Khan A, *et al*. Phaleria macrocarpa (Scheff.) Boerl. in Ethnopharmacology: Pharmacognosy, Safety, and Drug Development Perspectives. Prog Microbes Mol Biol 2024;7(1). Available from: http://hh-publisher.com/ojs321/index.php/pmmb/article/view/1080

9. Chelyn JL, Omar MH, Mohd Yousof NSA, Ranggasamy R, Wasiman MI, Ismail Z. Analysis of flavone C -glycosides in the leaves of clinacanthus nutans (Burm. f.) Lindau by HPTLC and HPLC-UV/DAD. Sci World J 2014 [cited 2019 Oct 1];2014:724267. Available from: http://www.ncbi.nlm.nih.gov/pubmed/25405231

10. Aslam MS. A review on phytochemical constituents and pharmacological activities of Euphorbia Helioscopia. Int J Pharm Pharm Sci 2015;(August):31–5. Available from: http://irjps.in/journal/47.pdf

11. Shim SY, Aziana I, Khoo BY. Perspective and insight on Clinacanthus nutans Lindau in traditional medicine. Int J Integr Biol 2013;14(1):7–9. Available from: https://www.researchgate.net/profile/Khoo-Boon-Yin/publication/266674852_Perspective_and_insight_on_Clinacanthus_nutans_Lindau_in_traditional_medicine/links/5436eb8a0cf2dc341db4c54f/Perspective-and-insight-on-Clinacanthus-nutans-Lindau-in-traditional-medi

12. Siew YY, Zareisedehizadeh S, Seetoh WG, Neo SY, Tan CH, Koh HL. Ethnobotanical survey of usage of fresh medicinal plants in Singapore. J Ethnopharmacol 2014;155(3):1450–66.

13. Khoo LW, Audrey Kow S, Lee MT, *et al*. A Comprehensive Review on Phytochemistry and Pharmacological Activities of Clinacanthus nutans (Burm.f.) Lindau. Evidence-based Complement Altern Med 2018 [cited 2019 Oct 14];2018:1–39. Available from: https://www.hindawi.com/journals/ecam/2018/9276260/

14. Alam A, Ferdosh S, Ghafoor K, *et al*. Clinacanthus nutans: A review of the medicinal uses, pharmacology and phytochemistry. Asian Pac J Trop Med 2016;9(4):402–9.

15. Babu S, Jayaraman S. An update on β-sitosterol: A potential herbal nutraceutical for diabetic management. Biomed Pharmacother 2020;131:110702. Available from: https://linkinghub.elsevier.com/retrieve/pii/S0753332220308957

16. Chanioti S, Katsouli M, Tzia C. β-Sitosterol as a functional bioactive. In: A Centum of Valuable Plant Bioactives. Elsevier; 2021. page 193–212.Available from: https://linkinghub.elsevier.com/retrieve/pii/B9780128229231000145

17. Khan SL, Siddiqui FA. Beta-Sitosterol: As Immunostimulant, Antioxidant and Inhibitor of SARS-CoV-2 Spike Glycoprotein. Arch Pharmacol Ther 2020;2(1). Available from:

https://www.scientificarchives.com/article/beta-sitosterol-as-immunostimulant-antioxidant-and-inhibitor-of-sars-cov-2-spike-glycoprotein

18. Morikawa T, Mizutani M, Aoki N, *et al*. Cytochrome P450 CYP710A Encodes the Sterol C-22 Desaturase in Arabidopsis and Tomato. Plant Cell 2006;18(4):1008–22. Available from: https://academic.oup.com/plcell/article/18/4/1008/6114851

19. Dampawan P, Huntrakul C, Reutrakul V, L. Raston C, H. White A. Constituents of Clinacanthus Nutans and the Crystal Structure of Lup-20(29)-ene-3-one. ScienceAsia1977;3(1):014. Available from: http://www.scienceasia.org/1977.03.n1/014.php

20. Bakrim S, Benkhaira N, Bourais I, *et al*. Health Benefits and Pharmacological Properties of Stigmasterol. Antioxidants 2022;11(10):1912. Available from: https://www.mdpi.com/2076-3921/11/10/1912

21. Panche AN, Diwan AD, Chandra SR. Flavonoids: An overview. J Nutr Sci 2016;5:e47. Available from: https://www.cambridge.org/core/product/identifier/S2048679016000410/type/journal_article

22. Zeng P, Zhang Y, Pan C, *et al*. Advances in studying of the pharmacological activities and structure–activity relationships of natural C-glycosylflavonoids. Acta Pharm Sin B 2013;3(3):154–62. Available from: https://linkinghub.elsevier.com/retrieve/pii/S2211383513000361

23. Charerntantanakul W, Kawaree R. Effects of medicinal plants extracts on interleukin-10 and tumor necrosis factor alpha gene expressions in porcine peripheral blood mononuclear cells. Chiang Mai Vet J 2010;8(2):93–103.

24. Nordin FJ, Pearanpan L, Chan KM, *et al*. Immunomodulatory potential of Clinacanthus nutans extracts in the co-culture of triplenegative breast cancer cells, MDA-MB-231, and THP-1 macrophages. PLoS One 2021 [cited 2022 Oct 6];16(8 August). Available from: /pmc/articles/PMC8357171/

25. Le CF, Kailaivasan TH, Chow SC, Abdullah Z, Ling SK, Fang CM. Phytosterols isolated from Clinacanthus nutans induce immunosuppressive activity in murine cells. Int Immunopharmacol 2017;44:203–10. Available from: http://dx.doi.org/10.1016/j.intimp.2017.01.013

26. Huang D, Guo W, Gao J, Chen J, Olatunji J. Clinacanthus nutans (Burm. f.) Lindau ethanol extract inhibits hepatoma in mice through upregulation of the immune response. Molecules 2015 [cited 2019 Oct 11];20(9):17405–28. Available from: http://www.mdpi.com/1420-3049/20/9/17405

27. Drioua S, Cherkani-Hassani A, El-Guourrami O, *et al*. Toxicological Review of Anticancer Plants Used in Traditional Medicine in Morocco. Prog Microbes Mol Biol 2023;6(1). Available from: https://journals.hh-publisher.com/index.php/pmmb/article/view/802

28. Ong YS, Tan LTH. Cancer, Natural Products and Nanodrug Delivery Systems. Prog Microbes Mol Biol 2020;3(1). Available from: http://hh-publisher.com/ojs321/index.php/pmmb/article/view/289

29. Thye AYK, Letchumanan V, Tan LTH, Law JWF, Lee LH. Malaysia's Breakthrough in Modern Actinobacteria (MOD-ACTINO) Drug Discovery Research. Prog Microbes Mol Biol 2022;5(1). Available from: http://journals.hh-publisher.com/index.php/pmmb/article/view/643

30. Abdou AG, Harba NM, Afifi AF, Elnaidany NF. Assessment of Cryptosporidium parvum infection in

immunocompetent and immunocompromised mice and its role in triggering intestinal dysplasia. Int J Infect Dis 2013 [cited 2019 Nov 11];17(8):e593–600. Available from: http://dx.doi.org/10.1016/j.ijid.2012.11.023

31. Surl CG, Kim HC. Concurrent response to challenge infection with Cryptosporidium parvum in immunosuppressed C57BL/6N mice. J Vet Sci 2006;7(1):47. Available from: https://vetsci.org/DOIx.php?id=10.4142/jvs.2006.7.1.47

32. Bachmanov AA, Reed DR, Beauchamp GK, Tordoff MG. Food intake, water intake, and drinking spout side preference of 28 mouse strains. Behav Genet 2002;32(6):435–43. Available from: http://www.ncbi.nlm.nih.gov/pubmed/12467341

33. Kaur A, Fang CM. An overview of the human immune system and the role of interferon regulatory factors (IRFs). Prog Microbes Mol Biol 2020;3(1). Available from: http://journals.hh-publisher.com/index.php/pmmb/article/view/338

34. Yu Y, Chen Y, Wang FL, Sun J, Li HJ, Liu JM. Cytokines Interleukin 4 (IL-4) and Interleukin 10 (IL-10) Gene Polymorphisms as Potential Host Susceptibility Factors in Virus-Induced Encephalitis. Med Sci Monit 2017;23:4541–8. Available from: https://www.medscimonit.com/abstract/index/idArt/904364

35. Laouini D, Alenius H, Bryce P, Oettgen H, Tsitsikov E, Geha RS. IL-10 is critical for Th2 responses in a murine model of allergic dermatitis. J Clin Invest 2003;112(7):1058–66. Available from: http://www.jci.org/articles/view/18246

36. Tonkonogy SL, McKenzie DT, Swain SL. Regulation of isotype production by IL-4 and IL-5. Effects of lymphokines on Ig production depend on the state of activation of the responding B cells. J Immunol 1989;142(12):4351–60. Available from: https://journals.aai.org/jimmunol/article/142/12/4351/21182/Regulation-of-isotype-production-by-IL-4-and-IL-5

37. Wang J, Ma L, Yang S, Wang S, Wei X, Song S. IL-10-Expressing Th2 Cells Contribute to the Elevated Antibody Production in Rheumatoid Arthritis. Inflammation 2016;39(3):1017–24. Available from: http://link.springer.com/10.1007/s10753-016-0331-5

38. Krautz C, Maier SL, Brunner M, *et al*. Reduced circulating B cells and plasma IgM levels are associated with decreased survival in sepsis - A meta-analysis. J Crit Care 2018;45:71–5. Available from: https://linkinghub.elsevier.com/retrieve/pii/S088394411731688X

39. Choi S, Kim TS, Lim HX. Lutein Suppresses the Maturation and Function of Bone Marrow-Derived Dendritic Cells. Prog Microbes Mol Biol 2024;7(1). Available from: https://journals.hh-publisher.com/index.php/pmmb/article/view/942

40. Calpe-Berdiel L, Escolà-Gil JC, Benítez S, *et al*. Dietary phytosterols modulate T-helper immune response but do not induce apparent anti-inflammatory effects in a mouse model of acute, aseptic inflammation. Life Sci 2007;80(21):1951–6. Available from: https://linkinghub.elsevier.com/retrieve/pii/S0024320507002068

41. Song B, Huang G, Tong C, *et al*. Gossypol suppresses mouse T lymphocytes via inhibition of NFκB,

NFAT and AP-1 pathways. Immunopharmacol Immunotoxicol 2013;35(5):615–21. Available from: http://www.tandfonline.com/doi/full/10.3109/08923973.2013.830126

42. Fisher WG, Yang PC, Medikonduri RK, Jafri MS. NFAT and NFκB Activation in T Lymphocytes: A Model of Differential Activation of Gene Expression. Ann Biomed Eng 2006;34(11):1712–28. Available from: https://link.springer.com/10.1007/s10439-006-9179-4

43. Lee JU, Kim LK, Choi JM. Revisiting the concept of targeting NFAT to control T cell immunity and autoimmune diseases. Front Immunol 2018;9(NOV). Available from: https://www.frontiersin.org/article/10.3389/fimmu.2018.02747/full

44. Leong CF, Ming LC, Aroua MK, Gew LT. Therapeutic and Pharmacological Role of Natural Products in Neurological Diseases: Targeting Autophagy Pathways. Prog Microbes Mol Biol 2025;8(1). Available from: http://journals.hh-publisher.com/index.php/pmmb/article/view/1118

45. Deng LJ, Qi M, Li N, Lei YH, Zhang DM, Chen JX. Natural products and their derivatives: Promising modulators of tumor immunotherapy. J Leukoc Biol 2020;108(2):493–508. Available from: https://academic.oup.com/jleukbio/article/108/2/493/6884482

46. Subroto T, Firdaus ARR, Kusumawardani S, *et al*. Homology Modeling and Expression of Recombinant NS5-RdRp Based on the Indonesian Local Strain of Dengue Virus for Anti-Dengue Drug Development. Prog Microbes Mol Biol 2024;7(1). Available from: https://journals.hh-publisher.com/index.php/pmmb/article/view/1031

47. Creasey HN, Zhang W, Widmer G. Effect of Caging on Cryptosporidium parvum Proliferation in Mice. Microorganisms 2022;10(6):1242. Available from: https://www.mdpi.com/2076-2607/10/6/1242

48. Gasparini SJ, Weber MC, Henneicke H, Kim S, Zhou H, Seibel MJ. Continuous corticosterone delivery via the drinking water or pellet implantation: A comparative study in mice. Steroids 2016;116:76–82. Available from: https://linkinghub.elsevier.com/retrieve/pii/S0039128X1630160X

49. Almutairi AB, Alshammari AAA, Rahmani AH, *et al*. Impact of Cyclosporine A on Cognitive Functions and Neuronal Oxidative Stress, Apoptosis and Inflammatory Markers in Rats. Prog Microbes Mol Biol 2024;7(1). Available from: https://journals.hh-publisher.com/index.php/pmmb/article/view/1039

50. Carter BL, Chalmers RM, Davies AP. Health sequelae of human cryptosporidiosis in industrialised countries: a systematic review. Parasit Vectors 2020;13(1):443. Available from: https://parasitesandvectors.biomedcentral.com/articles/10.1186/s13071-020-04308-7

51. Lacroix S, Mancassola R, Naciri M, Laurent F. Cryptosporidium parvum -Specific Mucosal Immune Response in C57BL/6 Neonatal and Gamma Interferon-Deficient Mice: Role of Tumor Necrosis Factor Alpha in Protection. Infect Immun 2001;69(3):1635–42. Available from: https://journals.asm.org/doi/10.1128/IAI.69.3.1635-1642.2001

52. El Hilaly J, Israili ZH, Lyoussi B. Acute and chronic toxicological studies of Ajuga iva in experimental animals. J Ethnopharmacol 2004;91(1):43–50.

53. Feng S, Dai Z, Liu A, *et al*. β-Sitosterol and stigmasterol ameliorate dextran sulfate sodium-induced colitis in mice fed a high fat Western-style diet. Food Funct 2017;8(11):4179–86. Available from:

https://xlink.rsc.org/?DOI=C7FO00375G

54. Feng S, Gan L, Yang CS, *et al*. Effects of Stigmasterol and β-Sitosterol on Nonalcoholic Fatty Liver Disease in a Mouse Model: A Lipidomic Analysis. J Agric Food Chem 2018;66(13):3417–25. Available from: https://pubs.acs.org/doi/10.1021/acs.jafc.7b06146

55. Pham LL, Watford SM, Pradeep P, *et al*. Variability in in vivo studies: Defining the upper limit of performance for predictions of systemic effect levels. Comput Toxicol 2020;15:100126. Available from: https://linkinghub.elsevier.com/retrieve/pii/S2468111320300360

56. Vilariño N, Louzao M, Abal P, *et al*. Human Poisoning from Marine Toxins: Unknowns for Optimal Consumer Protection. Toxins (Basel) 2018;10(8):324. Available from: https://www.mdpi.com/2072-6651/10/8/324